residue after precipitation of the primary mullite with free alumina (hydrargillite and diospore).

When estimating the degree or intensity of mullitization it is convenient to utilize the relative mullite yields, from the decrease in which the materials form the sequence: AR, NK, KhCC, ADC (Table 5).

*TABLE 5

DEGREE OF MULLITIZATION AT 1600°, %

Material	Al_2O_3	Total impurity oxides	Mullite yield		
			Theoretical (t)	Found (f)	Relative (f/t)
NK	44,30	3,50	61,71	58,00	0,94
AR	53,71	5,84	74,81	73,43	0,98
KhCC	55,25	4,22	76,96	68,97	0,90
ADC	62,00	4,87	86,36	51,17	0,59

• All commas are equivalent to a decimal point.

According to Table 5, the degree of mullitization of the materials, with the exception of AR, drops as the oxide impurity content in them increases. The Arkalyk rock, which takes first place in mullitization, is at the same time the richest in impurities (5.84%). This contradiction, however, is no longer valid when it is taken into account that the AR contains 4.48% titanium dioxides (see Table 1) which, like iron oxide, behaves differently in the sinters than the other impurity oxides. With the exception of $TiO_2 + Fe_2O_3$, the impurity content ($CaO + MgO + Na_2O + K_2O$) in the AR is 0.92% as opposed to 0.99% in the NK; in the KhCC it is 1.82%, and in the ADC it is 2.14%.

As a whole, the qualitative-quantitative phase transitions in the materials under consideration are predetermined during firing by the relationships between the chief components (SiO_2 and Al_2O_3) and the quantitatively secondary oxides, which, however, does not exclude the effect of other less important factors.

CONCLUSIONS

The stability of the phase composition of sintered material, essential for production processes, is achieved by firing at 1600° for a brief period.

Materials made of Novaya Selitsa kaolin, and particularly Arkalyk rock, of which very intensive mullitization is typical, are exceptionally valuable argillaceous components for charges for making high-alumina refractories by the present system of technology (on the basis of charges composed of refractory clays and commercial alumina).

ASSESSING STRUCTURE OF REFRACTORY PARTS

K. K. STRELOV
(Eastern Institute of Refractories)

The structure of refractory parts has a great effect on their properties and life.

The study of the structure of refractories and other ceramic parts follows two basic trends.

The first is the study of the structure in connection with the chemical and mineralogical composition. Here we investigate the microstructure and the composition and nature of the phase distribution. This trend has been called silicography (1), petrography or industrial stones (2), topoceramics (3), ceramography (4), physicochemical mechanics (5), and so on. The second trend is the study of the structure of refractory parts as porous bodies without any connection with their chemical and mineralogical composition. Here we are mainly concerned the microstructure or texture of the parts, i.e., the geometrical distribution of solid matter and pores.

The microstructure of a refractory as a porous body is most frequently described by the total content of open pores (apparent porosity); and more rarely the closed porosity and gas permeability. Pores, nevertheless, are extremely varied in size and shape and this has an effect on some of the properties of the parts. Hence this description of porosity is not always sufficient, on account of which new characteristics have been put forward:

The size and distribution of pores, the labyrinth factor, the channelling factor, the structure factor, the "referred" porosity, the shape and tortuousness factor, the specific surface of the pores (cm^2/cm^3), the boundary perimeter (mm/mm^2), and so on.

The size and distribution of pores. The commonest methods of determining the size of pores are based on the capillary equation $\underline{r} = \frac{2\sigma\cos\theta}{\rho}$, where $\underline{r}$ is the pore radius, ρ is the pressure, σ is the surface tension, and θ is the edge angle (6).

Two ways of capillarometry are applied: a) expulsion of the water from the saturated specimen by compressed air, and b) mercury porometers.

In the case where the pores are filled with water, $\cos\theta$ is taken as equal to unity. Several variations in the apparatus used for expelling the water with compressed air are known (7 - 11). The lower limit of the "resolving" power of these methods is about 3 microns, i.e., pores finer than 3 microns cannot be determined, hence this method is only applied for an approximate idea of the large pore size.

In the case of pores filled with mercury, $\cos\theta$ is less than unity. The instruments used, mercury prometers, also vary in design (12, 13 and 14).

The Soviet Union uses two types of porometers - high and low pressure ones - to determine the size of pores ranging from several Angstrom units to several millimeters.

The high-pressure porometers designed by the Leningrad Technological Institute (13), and the Grozno Oil Institute (14) are used to determined pores from 30 Å to 5 microns. The Berkman porometer (15) determines pores from 1 - 5 microns

to 1 mm. The applicability of mercury porometers to pores in refractory materials has been established by a large amount of research (16, 17).

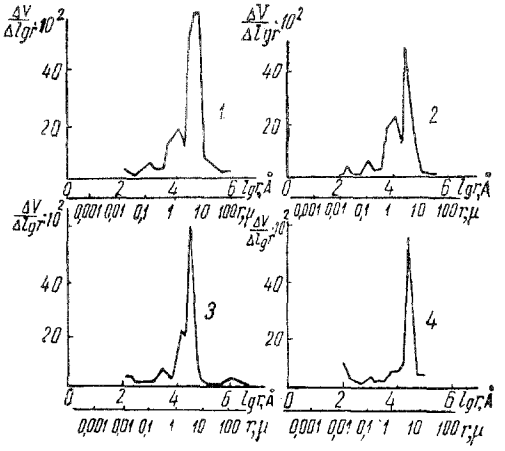

Fig. 1. Differential curves showing distribution of pores plotted from results of tests with mercury porometer (description of specimens in Table 1)

The results of determination of pore size with mercury porometers can conveniently be shown in the form of differential and integral curves. The differential curves within the coordinates $\Delta V/\Delta \log r$ - $\log r$, where ΔV is the increment in the mercury volume entering the specimen with a corresponding increment in the logarithm of the radius $\Delta \log r$, are frequency curves. In these curves (Fig. 1) we can observe one or several maxima corresponding to pores of the commonest dimensions. The integral curves within the coordinates V - $\log p$ or V - $\log r$, where V is the total (increasing) volume of mercury (in % of the volume) entering the specimen at the corresponding pressure p, show the distribution of pores according to size (Fig. 2).

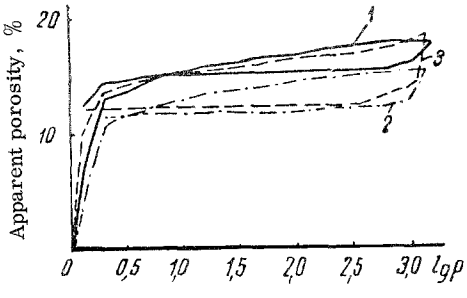

Fig. 2. Integral curves for chamotte specimens (ladle brick with porosity 17%): 1 — in the initial state; 2 — after firing at 1500°; 3 — after 3 heating-cooling cycles (1200 - 50°)

Integral curves recorded when the pressure rises or falls form a peculiar "hysteresis loop", the shape of which leads us to certain conclusions with regard to the pore shape.

These methods enable us to study the morphology of pores and to establish the relationship between their size and the technological production factors, as well as the properties of the parts.

Labyrinth factor. The labyrinth factor has been put forward on the basis of the following consideration (18). When they join together, open pores sometimes form intricately shaped channels with a large number of dead-end branches, converging and diverging sectors, and so on.

If a liquid or gas flows through a porous body in a certain direction, despite the fact that the entire volume of open pores will be filled, only part of the liquid or gas will actually be in motion. The remainder, becoming locked in the dead-end pores, "sacks", "dead spaces", and so on, hardly takes part in the motion.

When considering the corrosive effect of an aggressive agent, apart from the total extent of open porosity, it is important for us to know the number of pores through which there is motion and renewal of the melt or gas.

The volume of open pores through which the liquid or gas may move is called the permeable or effective porosity (ϵ_{ef}). The ratio of the effective porosity to the total has been called the labyrinth factor $X = \epsilon_{ef} : \epsilon_o$.

The equation for the permeable or effective porosity is derived on the basis of Poiseuille's law (19, 20):

$$\varepsilon_{ef} = 8\Gamma_a : r^2_{ef},$$

where r_{ef} is the radius of the permeable pores in m; Γa is the absolute gas permeability in m^2.

The gas permeability factor k ($1 \cdot m/m^2 \cdot hour \cdot mm\ H_2O$), determined from OST MKTP 4312, can be converted to absolute gas permeability Γa by the formula $\Gamma a = 0.51 \cdot 10^{-12} k$.

The difficulty in determing ϵ_{ef} lies in the need to establish the correct values of r_{ef}, for which two ways can be put forward.

In the first method the radius of the permeable pores is determined by one method as r_{min} (7 - 11).

In these methods, when the water is expelled from the pores in the sample by compressed air, r_{min} is calculated from the point at which the curvilinear sector of the relationship "flow - pressure" changes to a rectilinear sector. The reason for the appearance of the rectilinear sector, as shown earlier (21), may be the inadequacy of the applied pressure. It is clear that the equality $r_{ef} \approx r_{min}$ is of a conditional nature.

The other way to determine r_{ef} is to find the size of the pores by filling them with mercury under pressure.

The size of the pores corresponding to the maximum on the differential curve is taken as r_{ef}. When there are several maxima onthe differential curves, it is not possible to determine r_{ef} by these methods.

Table 1 shows the results of the calculation carried out by both methods, and Figs. 1 and 3 show the relevant curves.

Comparison of the results suggests that in the given case fairly close figures can be obtained by both methods for the pore dimensions.

The derived values for the labyrinth factor for different refractory parts range from 0.1 to 0.76 (Table 2).

Channelling factor. Just as the labyrinth factor, the channelling factor shows the number of pores through which a liquid or gas may flow, but, as distinct from the labyrinth factor, it only takes into account the large permeable pores, for example, those greater than 2.5 microns (in radius); this factor is easily calculated (21).

When the water is expelled from the saturated specimen by compressed air (11) at 450 mm Hg, the water is forced out of permeable pores with a "radius" larger than 2.5 microns, but is left in the impermeable (dead-end pores, "sacks", "dead" spaces, water films, and so on) and open pores with a "radius" less than 2.5 microns. The number

TABLE 1

COMPARATIVE RESULTS OF DETERMINING SIZE OF PORES OF CHAMOTTE SPECIMENS *

No. of specimen	Apparent porosity, %	Method of calculation, pore radius		
		expulsion of water by compressed air [11]		Forcing in mercury, microns
		pressure in mm Hg	r_{min} microns	
1	28,9	200	5,5	6,3
2	25,9	500	2,2	**2,5**
3	27,5	455	2,4	**3,1**
4	29,8	550	2,0	**3,1**

* All commas are equivalent to a decimal point.

of permeable pores larger than 2.5 microns (in % or fractions of unity) has been called the channelling porosity, and the ratio $\epsilon_{ch}:\epsilon = k$ is the channelling factor.

Channel porosity is calculated from the formula

$$\varepsilon_{ch} = \frac{a_1 - a_2}{V} 100, \%,$$

where a_1 is the weight of the specimens saturated with water (prior to the experiment), g; a_2 is the weight of the specimens after the experiment, g; and V is the volume of the specimen in cm^3.

The pressure 450 mm Hg is taken conditionally. It could probably be increased, which would make it possible to determine the channelling for smaller permeable pores.

The channel porosity of chamotte parts does not depend upon apparent porosity and gas permeability, but is an independent characteristic of the pore's structure (Figs. 4 and 5).

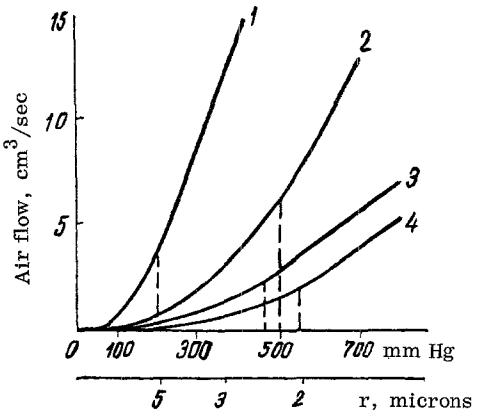

Fig. 3. Consumption of air as function of pressure. The pressure corresponding to the beginning of the rectilinear section of the curves is used to determine the minimum radius of permeable pores (description of specimen given in Table 1)

Its values range from 0.148 to 0.764. The channelling and labyrinth factors do not coincide.

Classification of porosity, making allowance for permeable and channel porosity, can be represented in the form of the diagram in Fig. 6.

Structure factor, (23, 24 and 25). A porous body is regarded as a "mixed body" consisting of solid material and air. On the basis of the theory of mixed bodies we can derive the relationship:

$$\frac{Y}{Y_1} = \frac{kX_1}{k + (1 - X_1)},$$

where Y is the measured "conduction power" of the mixed body; Y_1 is the corresponding power of the solid material; X_1 is the bulk fraction of the solid material, and k is the

TABLE 2

POROSITY INDICES FOR SOME REFRACTORIES (22) *

Part	Porosity, fractions of unity			Labyrinth factor $X = \frac{\varepsilon_{ef}}{\varepsilon_0}$	Structure factor $k = \frac{X(1-\varepsilon_0)}{1-X}$	Specific surface $S_V = \sqrt{\frac{\varepsilon^5}{k_1 r_a}}$, cm^2/cm^3
	Open (apparent), ε	Total, ε_0	Permeable (effective), ε_{ef}			
Open-hearth dinas, specific gravity 2.36 — 2.42	0,15	0,18	0,10	0,56	1,05	789
Coke dinas specific gravity 2.33 — 2.38	0,26	0,32	0,05	0,14	0,11	635
Magnesite	0,17	0,20	0,05	0,24	0,25	369
Chrome-magnesite	0,21	0,26	0,06	0,24	0,23	478
Sillimanite about ~63% Al_2O_3	0,17	0,21	0,04	0,17	0,16	1066
Chamotte with the following Al_2O_3 content, %:						
40 — 42	0,17	0,18	0,08	0,44	0,65	640
44	0,14	0,17	0,06	0,32	0,39	1059
36—39	0,23	0,26	0,05	0,19	0,17	456
32—35	0,25	0,27	0,16	0,59	1,05	614

* All commas are equivalent to a decimal point.

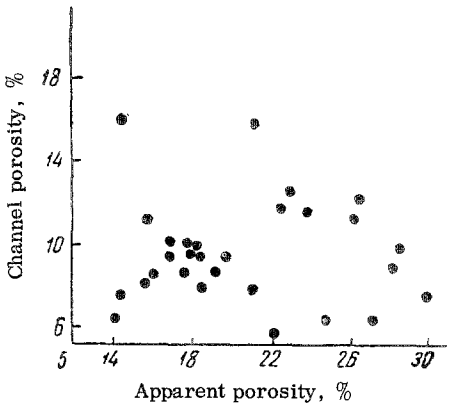

Fig. 4. Relationship between channel porosity and apparent porosity in chamotte parts

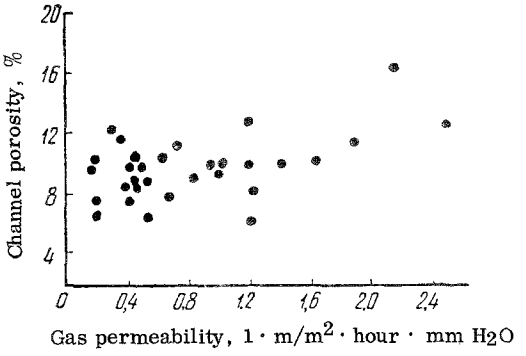

Fig. 5. Relationship between channel porosity and gas permeability in chamotte parts

structure factor.

The structure factor k is related to the labyrinth factor X in the following way

$$k = \frac{X(1-\varepsilon_0)}{1-X}.$$

The structure factor has an infinite value when almost all the pores are permeable (1 - X) $\to$ 0, and is equal to zero when there are no permeable pores, X $\to$ 0. A less permeable structure corresponds to a lower factor, and vice versa. The structure factor and its relationship with the other porosity indices is shown in Table 2.

"Referred" porosity. The "referred" porosity (26) describes capillary attraction; it is determined in the same way as the apparent porosity, but the specimen is boiled in water during the process and not in a vacuum[1]. The "referred" porosity of chamotte parts in the manufactured state is a definite function (Fig. 7) of the apparent porosity (calculated with correlation factor - 0.95). After secondary firing at 1500° the link between "referred" and apparent porosity weakens (correlation factor 0.344).

In the case of some high-fired and dense parts, the referred porosity is proportional to the apparent porosity and does not differ to any great extent in size. In this respect it may be regarded as an independent characteristic of the porous structure.

Specific surface and mean pore radius. In order to determine the surface of pores per unit of volume two different methods have been put forward (cm²/cm³).

The first method is based on the idea of a mean pore radius: $S = \frac{2\epsilon}{r_{mean}}$ cm²/cm³, where ϵ is the open (apparent) porosity in fractions of unity; r_{mean} is the mean radius of the open pores in cm; S is the specific surface of the open pores, cm²/cm³.

Another method has been suggested by Carman (27). He has suggested a formula in the following form:

$$S_V = \sqrt{\frac{\varepsilon_0^3}{k_1 \Gamma_a}}\ см^2/см^3,$$

where ϵ_0 is the total porosity in fractions of unity; k_1 is the Coseni factor, a constant equal to 5 $\pm$ 0.5; Γa is the absolute gas permeability in m².

The following formula is used for the calculation [2]

$$S_V = 6{,}25\sqrt{\frac{\varepsilon^3}{k}}\ см^2/см^3,$$

where S_V is the specific surface of the pores in cm²/cm³; ϵ is the apparent porosity in %, k is the gas permeability factor in 1 · m/m² · hour · mm H_2O.

We will show the link between the two formulae for the specific surface without deriving Carman's formula here.

We will make the following transformations in Carman's formula: let us replace Γa by its developed form, let us take the coseni factor as 5, let us denote ϵ_{ef} in terms of total porosity ϵ_0 and the labyrinth factor X.

After this we obtain $S_V = \frac{\varepsilon_0}{r_{ef}} \cdot \frac{1{,}264}{\sqrt{X}}$.

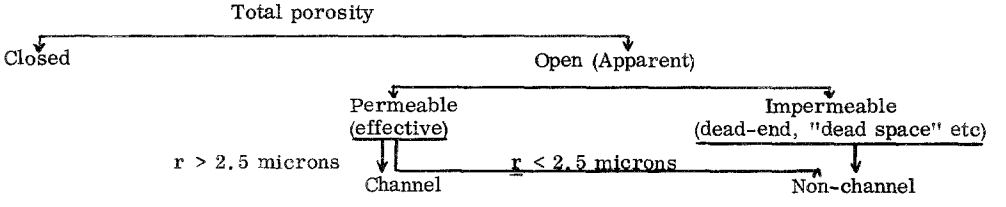

Fig. 6. Classification of porosity

[1] From the editors: The water absorption of most constructional ceramic parts is determined in similar fashion (in the cold state). The ratio of the cold water absorption to the hot (or the ratio of the referred porosity to the apparent porosity, which is the same thing) is sometimes used as an index for the structure of constructional ceramic parts, in particular, for their frost resistance.

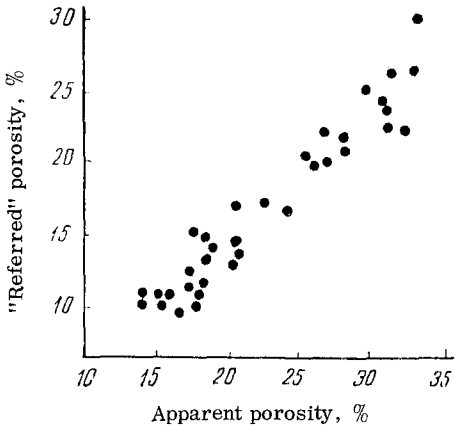

Fig. 7. Relationship between "referred" porosity and apparent porosity in chamotte parts

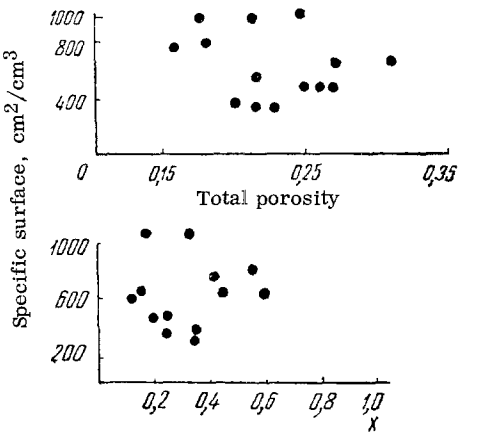

Fig. 8. Relationship between specific surface of different refractories and total porosity and labyrinth factor

If we take it that $\epsilon_0 \approx \epsilon$, $r_{ef} \approx r_{mean}$, and take the extreme values of X, than at X = 1, S = 1.88 S_V; at X = 0.1, S = 0.5 S_V.

Thus, for a rough evaluation we can use both methods for determining the specific surface, but in quoting the results we will have to point out the method used to derive them[3].

The specific surface is not a function of the labyrinth factor or the total porosity (Fig. 8).

The values of the specific surface for some of the refractories are given in Table 2.

Comparing two expressions for the specific surface and taking $S = S_V$, it is possible to determine the mean pore radius[4];

$$r_{mean} = 32\sqrt{\frac{k}{\epsilon}} \text{ microns}$$

where r_{mean} is the mean pore radius in microns; k is the gas permeability factor in 1 · m · /m² · hour · mm H_2O, and ϵ is the apparent porosity in %.

This formula is similar to Kustov's (19).

Pore boundary perimeter. The perimeter of the pore boundary (mm/mm²), just as the specific surface (cm²/cm³), describes the size of the pores and the number of them. A method for deriving the boundary perimeter has been worked out and is applied in metallography (28, 29). The calculation itself consists in calculating the transition points "solid body - pore" for a large number of arbitrarily chosen directions in sections under a microscope.

The derived values of the pore perimeter for chamotte parts range from 4.5 to 43.9 mm/mm² and, as can be seen from Fig. 9, are not a function of the total porosity.

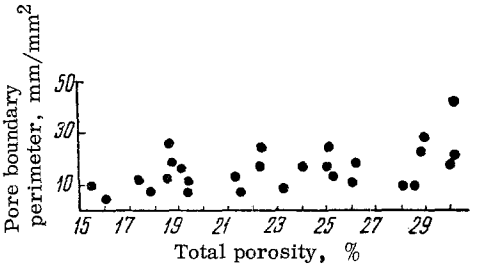

Fig. 9. Relationship between boundary perimeter and total porosity of chamotte parts

CONCLUSIONS

The methods of determining pore size, channelling and "referred" porosity, specific surface and boundary perimeter make it possible to obtain fairly reproducible results, which in principle enables us to use them for a comparative description of the structure of different refractory materials.

The theoretical formulae for determining the labyrinth factor, the structure factor and so on are less perfect and are therefore restricted in use.

At the present time there is comparatively little data available on the relationship between the porosity and the most important properties of refractories or their behavior in service. The accumulation of relevant material is an

---

2) If we do not take into account the coseni factor when deriving the formula for specific surface, but substitute r into the elementary formula S = 2 ϵ/r instead, deriving r from the Poiseuille equation $r = \sqrt{\frac{8\Gamma_a}{\epsilon}}$, then the specific surface formula takes the form: $S = 10\sqrt{\frac{\epsilon^3}{k}}$, where S is cm²/cm³; ϵ - %; k - 1 · m/m² · hour · mm H_2O.

3) From the editors: Besides the ways of calculating the specific surface mentioned by the author, the low temperature nitrogen adsorption method is also interesting. This method makes it possible to determine the entire open pore surface more accurately, including the very fine, labyrinth and other type pores, through which the gas stream hardly passes at all.

4) If we substitute ϵ in % into the formula resulting from the Poiseuille equation $r = \sqrt{\frac{8\Gamma_a}{\epsilon}}$ microns, and express Γa in terms of k, we obtain $r = 20\sqrt{\frac{\kappa}{\epsilon}}$ microns.

urgent task in the investigation of the porous structure of refractories.

REFERENCES

1. I. F. Ponomarev. Papers of Second Conference on physico-chemical analysis, 1933.
2. D. S. Belyankin, B. V. Ivanov, V. V. Lapin. Petrography of commercial stone, 1952.
3. Gijn, Brit. Ceram. Soc., 1954, No. 10, 53.
4. Ryshkevich, Collection of translation of "Chemical and technology of silicates", 1956, 3.
5. P. A. Rebinder. Physico-chemical mechanics, 1958.
6. H. Bechhold. Z. phys. chem., 1908, 64.
7. Ye. V. Merkulova. Development of method of calculating pore size and distribution in refractory materials. VNIIO (Kharkov), 1954.
8. V. V. Stender. Diaphrams for electrolysis of warm water solutions, 1948.
9. I. Ya. Shikin, M. G. Koganer. Oxygen, 1949, No. 2.
10. L̆agar. Parch. Eisenhüttenwesen, 1955, No. 9, 26
11. K. K. Strelov. Zavodskaya Laboratoriya, 1956, No. 12.
12. H. L. Ritter, L. C. Drake, Ind. Eng. Chem. Anal. Ed. 1945, 17.
13. T. G. Plachenov, V. A. Aleksandrov, G. N. Belotserkovskiy and N. M. Kamakin. Methods of investigating the structure of highly-dispersed and porous bodies. Conference papers, 1953.
14. Reference missing from Russian text.
15. A. S. Berkman, ZhPKh, 1957, V. XXX, issue 6.
16. K. Konopisky, W. Lohre. Ber. Deutsch. keram. Ges. 1956, No. 4.
17. L. Lecrivain. Trans. Brit. Ceram. Soc., 1958, No. 11.
18. E. Manegold. Kolloid Z., 1938, 82.
19. B. I. Kustov. Ogneupory, 1949, No. 6.
20. L. Žagar. Archiv. Eisenhüttenwesen, 1955, No. 12, 26.
21. K. K. Strelov, I. P. Duvalova. Ogneupory, 1959, No. 3.
22. L. Žagar. Archiv. Eisenhüttenwesen, 1956, No. 10,27.
23. K. Torkar. Oster. Chemiker-Ing., 1952, 53.
24. K. Torkar. Chem.-Ing.-Tchan., 1953, 25.
25. K. Torkar. Ber. Deutsch. Keran Ges. 1954, No. 5.
26. A. C. Frenkel'. Ogneupory, 1956, No. 8.
27. P. C. Carman. Trans. Inst. Chem. Eng., 1937, No. 15; Trans. Farad. Soc., 1954, No. 50.
28. S. A. Saltykov. Introduction to stereometric metallography, 1950.
29. Ye. Ye. Levin. Microscopic investigation of metals, 1955.

INTERACTION BETWEEN CHROMITE AND MAGNESIUM OXIDE WHEN HEATED

S. M. ZUBAKOV
(Institute of Metallurgy and Benefication of the AS of the Kazakh SSR)

A study was made earlier of the reactions in the solid state between Akkarga chromite ore and magnesium oxide in chrome-magnesite mixtures of the heat-resistant type (1 - 3).

When these mixtures are fixed, complex diffusion processes develop at the contact points between the chromite and periclase grains and form reaction edges (4).

The peculiar zonality of the structure of the heat-resistant chrome-magnesite refractory (5), which shows up as the alternation of the phase composition typical of chromite, chrome-magnesite and magnesite compositions, must be taken into account when evaluating and studying its chemical-mineralogical composition. In minealogical composition this refractory should be regarded as a combination of chromite, chrome-magnesite and magnesite brick.

As initial raw material for the investigation we used Saranov and Kimpersay chromite ores and chemically pure magnesium oxide. The latter was pre-pressed into compacts, fired at 1600° and ground down into two fractions 1 - 0 and 0.06 - 0 mm.

The chemical composition of the initial materials is given in Table 1. The weight composition of the charge was 50% chromite ore 1 - 3 mm and 50% periclase powder 1 - 0 mm. For purposes of comparison we also prepared a charge from fine-ground materials with a grain size less than 0.06 mm.

The results of the investigation of the finely-ground mixtures may be important for the development of technology in the production of periclase-spinel brick.

The mixtures were moistened with sulfite alkali with a density 1.12 and allowed to stand for a day. Specimens were pressed at 1000 kg/cm2, fired at 1680° for four hours in a mildly oxidizing medium.

To gain an idea of the degree of variation in the chrome spinel composition during firing, the powders with a fraction finer than 30 microns were examined through a microscope against the light, and the number of translucent and non-translucent crystals counted.

In the coarse-ground mixtures, the chromite grains were not firmly linked with the periclase, which made it possible to separate them and examine them independently. The thoroughness with which the chromite grains had been separated from the periclase grains surrounding them was checked under the microscope.

The results of the chemical analysis, microscopic and x-ray investigation of the chrome-magnesite specimens, and the chromite and periclase grains separated from the coarse-ground mixtures are given in Tables 2 and 3.

When coarse-ground chrome-magnesite mixtures are